J. Fluid Mech. (1986), *vol.* 172, *pp.* 33–46
Printed in Great Britain

Sensitivity of transition phenomena to small perturbations in flow round a circular cylinder

By GÜNTER SCHEWE
DFVLR – Institut für Aeroelastik (AVA), Göttingen, D-34 Göttingen, West Germany

(Received 2 September 1985 and in revised form 7 May 1986)

In the critical Reynolds-number range ($Re = 3–4 \times 10^5$) the structure of the flow around a circular cylinder undergoes drastic changes that are coupled with a break in symmetry manifested by the occurrence of a steady lift force having unpredictable sign. Between the stable states the time functions of lift exhibit chaotic behaviour. Sensitivity to small perturbations is demonstrated by experiments showing that in principle it is possible to trip all transition jumps in the critical range by a perturbation localized in space and time. The structural changes of the flow, in particular the symmetry breaks, are visualized by oil-flow photographs. Furthermore the transition jumps were recorded in the time domain, thus the characteristic time for the jumps was obtained.

1. Introduction

A typical characteristic of nonlinear systems is their sensitivity to perturbations in critical situations. One consequence of this sensitivity is, for example, that transitions between individual stable states can, near a critical point, be influenced or controlled by a very small perturbation which may be natural or artificial. In this paper we shall demonstrate this sensitivity by experiments in which transition from laminar to turbulent flow is tripped by a perturbation localized in space and time. In general, the experiments will demonstrate that there are situations in which events in the microstructure can cause changes in the macrostructure of a system.

The common techniques for initiating transition from laminar to turbulent flow use large perturbations such as trip wires or strips. Consider, for example, the classical experiment by Prandtl (1914) which involved forced transition from laminar to turbulent flow around a sphere. Since this perturbation consisted of a wire around the sphere, the length of the extended trip wire and diameter of the sphere are of the same order. We shall show that transition can be initiated by a perturbation that is small in comparison with the spatial extent of the flow configuration and the shed vortices.

We have previously reported on a symmetry-breaking instability occurring in flow round a circular cylinder (Schewe 1983*a*). Within the range of critical Reynolds number ($Re \approx 3–4 \times 10^5$) when the drag coefficient C_D declines rapidly, we observed steady asymmetric flow states manifested by steady lift forces having unpredictable sign and jumps in the Strouhal number. The break in symmetry, i.e. the asymmetric flow states, can be explained by the fact that transition from laminar to turbulent flow in the boundary layer occurs first on one side of the cylinder and then, at a slightly higher Reynolds number, on the other side. The discontinuous jumps between individual states can be interpreted as subcritical bifurcations.

With regard to jumps in the vortex-shedding frequency, we found experimentally that the ratio of Strouhal numbers belonging to different stable states is nearly

constant and corresponds approximately to the 'Golden Section' (or 'Golden Ratio' $G = \frac{1}{2}(\sqrt{(5)}+1) = 1.6\ldots$; Schewe 1985*a*).

To explain the unpredictability in the sign of the lift force, we assumed (Schewe 1983*a*) that the side of the cylinder where transition first occurs is determined by events in the microstructure of the flow. This being the case, it is therefore conceivable that transition can be initiated at a critical point by local perturbations or fluctuations inherent in the flow which occur stochastically in both space and time. Thus, the sign of the lift force may be dependent upon the side of the cylinder on which a perturbation sufficient to initiate transition first occurs.

To test these speculations, we simulated the above-mentioned small perturbation with one artificial local inhomogeneity on the surface of the circular cylinder. In Schewe (1983*b*), we first reported that it is possible to trip all transitions within the range of critical Reynolds numbers with a small movable pin. We shall give a more detailed description of these experiments in the present paper, and provide additional information on the phenomena which take place within the range of critical Reynolds numbers. We took oil-flow photographs in order to visualize the individual states. Furthermore, by directly measuring transition jumps in the time domain, we collected data on the characteristic times of these transition jumps.

2. Experimental arrangement

Experiments were performed in the same pressurized wind tunnel in Göttingen and, in most cases, with the same circular cylinder described in Schewe (1983*a*, *b*). With the exception of the flow-visualization experiments, the flow speed lay within the range $U_\infty = 10$–20 m/s, which means that the range of critical Reynolds numbers was reached at a pressure of $p = 6$ bar. In this range of critical Reynolds numbers, turbulence intensity was about $Tu = 0.3\,\%$. The closed square test section of the wind-tunnel measures 0.6×0.6 m^2. With a diameter of $D = 0.06$ m and a length of $L = 0.6$ m, the circular cylinder has an aspect ratio of $L/D = 10$, and produces a 10 % geometric blockage of flow in the tunnel. The polished cylinder has a roughness of about $k = 1$ μm, which yields a non-dimensionalized roughness parameter of $k/D \approx 10^{-5}$. In several cases we used a more slender cylinder with a diameter of $D = 0.034$ m, which yields an aspect ratio of $L/D = 18$ (geometric blockage: 5.7 %). We used this more slender cylinder for the flow-visualization experiments because it was easier to dismantle when taking photographs.

The flow was studied by measuring steady as well as unsteady forces acting on the cylinder. The balance, which operates with 3-component piezoelectric force transducers (Kistler model 9067), has been described by Schewe (1983*a*, 1985*b*). A major feature of this balance is its high stiffness which results in a high natural frequency and low levels of interference between the individual force components. Furthermore, the balance is characterized by a large dynamic range, even for quasi-static measurements ($1 \lesssim F \lesssim 10$ kN), and a threshold of 0.01 N for measurements of unsteady forces. The signals were evaluated with a Nicolet 660B analyser and a computer equipped with an analog–digital converter system.

3. Results

We shall first consider the functional relationship between the drag coefficient C_D and the Reynolds number Re shown in figure 1. In this figure we have collected the classical measurements of Wieselsberger (1923), which represent the lower range of

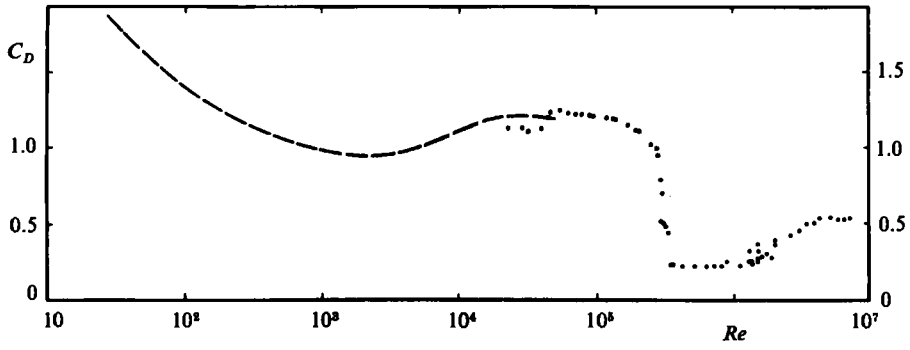

FIGURE 1. Drag coefficient C_D versus Reynolds number: ---, Wieselsberger (1923); · · · · · ·, Schewe (1983*a*). The most drastic change in C_D occurs in the critical range ($Re \approx 3 \times 10^5$). This paper concentrates on phenomena occurring in this regime.

Re, and our measurements (Schewe 1983*a*), representing the higher range. The most obvious change in $C_D(Re)$ occurs in the critical Reynolds-number range $3\text{–}4 \times 10^5$, where C_D falls from its subcritical value of 1.2 to the supercritical value of 0.2. This decline of C_D (often called drag crisis) is a consequence of drastic changes in the global structure of the entire flow field.

3.1. *Flow visualization of structural changes*

In order to gain a visual impression of the changes in the global structure occurring in individual states, we took oil-flow photographs of time-averaged skin-friction lines. Since the oil suspension itself would increase the surface roughness of the cylinder, an indirect method was chosen so that the cylinder would not be affected by the visualization method. We therefore photographed only the skin-friction lines on the walls of the test section between which the cylinder was mounted. The topological structure of the flow near the wall is very complicated. Flow in this region is determined by interference effects between the so-called horseshoe vortex wrapped around the cylinder and the boundary layer on the wall. In spite of these complications, however, certain conclusions can be drawn concerning the mean flow field around a cylinder. Details of the flow in the vicinity of the sidewalls differ considerably from those in the centre of the span. Nevertheless the streamline pattern on the wind-tunnel walls does serve as an indication of global changes in the nominally two-dimensional flow around the cylinder. Figures 2(*a–e*) show the photographs taken at different Reynolds numbers in and near the critical regime. The flow speed was approximately $U_\infty = 31$ m/s in all four cases; the Reynolds number was changed by varying the pressure in the wind tunnel. Both oil-flow pictures and force measurements were made during the same runs.

It is obvious from the results that, depending on the Reynolds number, there is a drastic change in the global structure of the individual states. The photograph in figure 2(*a*) was taken at $Re = 2 \times 10^5$ (subcritical $Re/Re_{c_1} \approx 0.66$) where the mean flow is symmetric ($C_L = 0$) and characterized by quasi-periodic vortex shedding with Strouhal number $Sr = 0.2$ and by $C_D = 1.1$. For the result shown in figure 2(*b*), the Reynolds number was adjusted to be as near as possible to the first critical value Re_{c_1} which occurs just prior to transition in the asymmetric state. Figures 2(*c, d*) show the break in symmetry, i.e. they show both possible asymmetric flow states where $C_L = -1.1$ (figure 2*c*), $C_L = +1.1$ (figure 2*d*), $C_D = 0.5$, and $Sr = 0.3$. The pictures

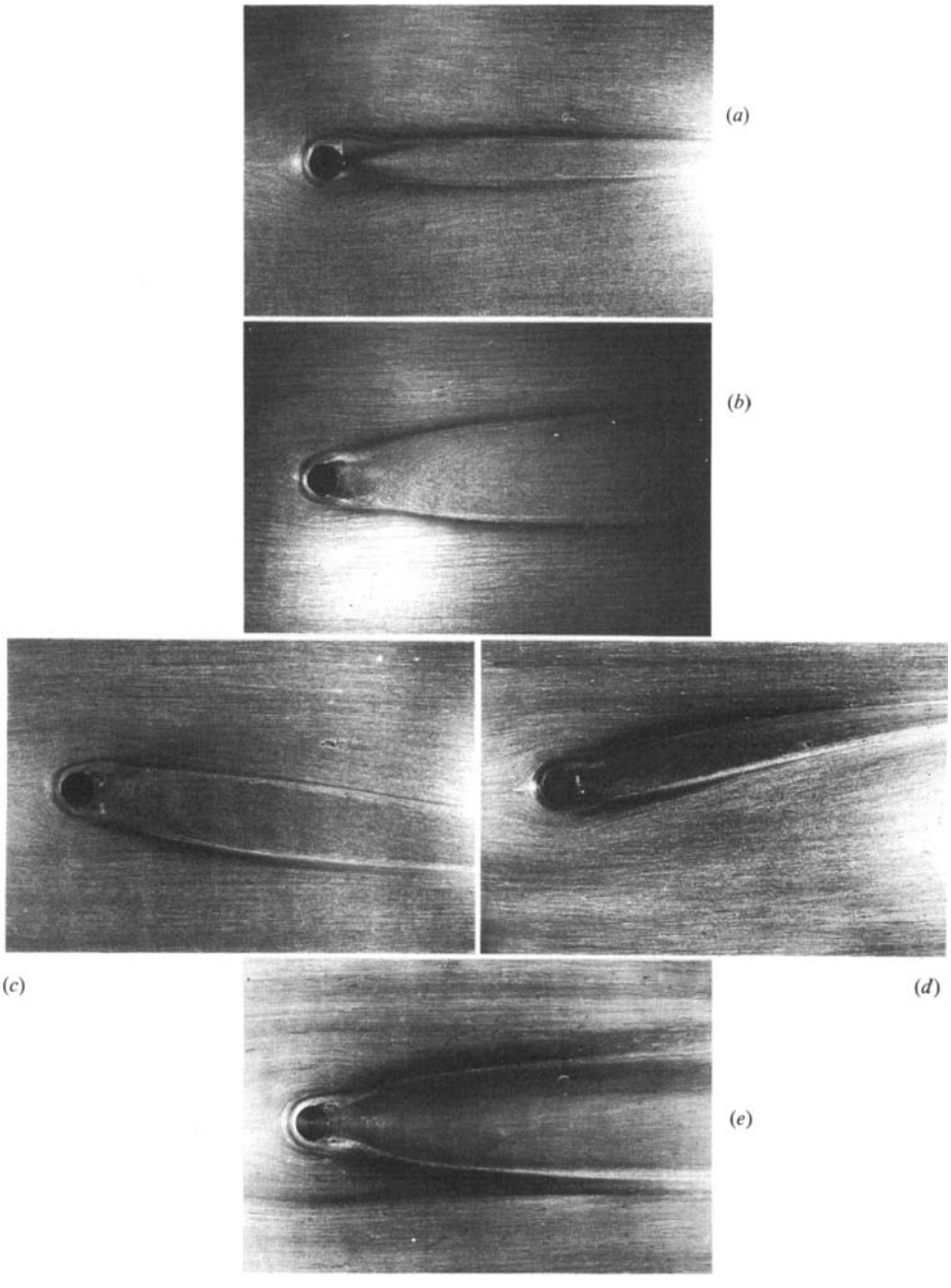

FIGURE 2. Oil-flow photographs taken from the sidewalls between which the cylinder is spanned. The pictures provide footprints of the structural changes dependent on the Reynolds number. (*a*) Subcritical symmetric state $Re = 2 \times 10^5$; (*b*) symmetric state immediately before the first transition jump $Re_{c_1} = 3 \times 10^5$; (*c*; *d*) both possible asymmetric states after the transition $Re_{c_1} = 3 \times 10^5$; (*e*) symmetric supercritical state $Re = 4 \times 10^5$.

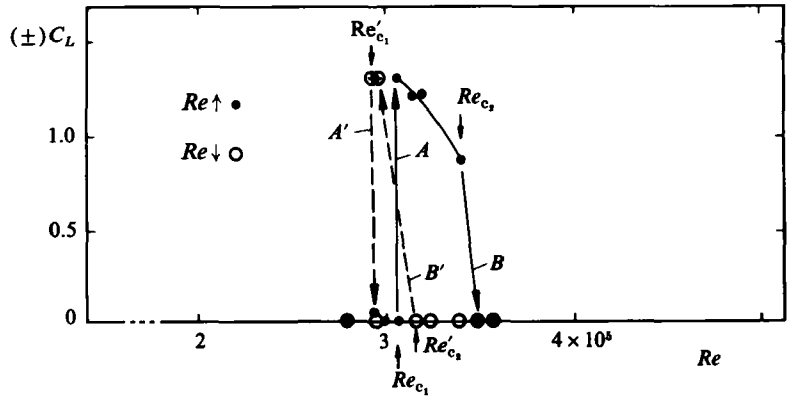

FIGURE 3. Behaviour of the steady lift coefficient C_L in the critical Re range. At the critical values Re_{c_1} and Re_{c_2} the transition jumps A and B occur for increasing Re ($Re\uparrow$). Owing to hysteresis the corresponding jumps for decreasing Re ($Re\downarrow$) B' and A' occur at Re'_{c_2} and Re'_{c_1}. The sign of C_L is unpredictable. The transition jumps are coupled with a small change ϵ in Re due to feedback effects on the incoming flow. Therefore the transition jumps are not vertical ($\epsilon = 0$), as would be the case under ideal conditions (see also Schewe 1983*a*).

in figures 2(*c*, *d*) were taken at approximately the same Reynolds number $Re_{c_1} = 3\times10^5$ after the first transition (A) had occurred. Conclusions regarding the sign of the lift force can be drawn from the location of the stagnation points on the front of the cylinder. With respect to the centreline in figure 2(*c*), the stagnation point is shifted to the upper side of the cylinder, while in figure 2(*d*) it is shifted to the lower side. These shifts result in a negative and a positive lift respectively. Under ideal conditions, the pictures in figures 2(*c*, *d*) would be mirror images of each other at the centreline.

Figure 2(*e*) represents the supercritical state at $Re = 4\times10^5$, where the mean flow field is again symmetric ($C_L = 0$) and $C_D = 0.2$; the Strouhal number here is 0.48. The fact that C_D and C_L, which were measured simultaneously with the flow visualization, differ slightly from the values given in figure 1 and in the following figure 3 is caused by different blockage effects in the two cases. In the five pictures we can see moderately dark traces which are probably flow-separation lines caused by the horseshoe vortex formed at the junctions between the cylinder and the wind-tunnel walls. These lines should not be interpreted as a quantitative measure of the wake width, however. We should emphasize again that the purpose of showing these photographs is only to provide additional documentation of the break in symmetry as well as of the changes that occur in the global structure when the flow goes from the subcritical to the supercritical state. From the point of view of this paper, the complicated behaviour of the flow at the wall is a secondary effect. Nevertheless, the flow patterns on the wind-tunnel walls have provided footprints of changes in the global flow structures.

3.2. *Description of the phenomena*

Before proceeding to the experiments with artificial local perturbations of the flow, it will be useful to re-examine previously published observations (Schewe 1983*a*, *b*) using improved representations and adding additional results.

Figure 3 shows the behaviour of the steady lift coefficient C_L in and near the critical

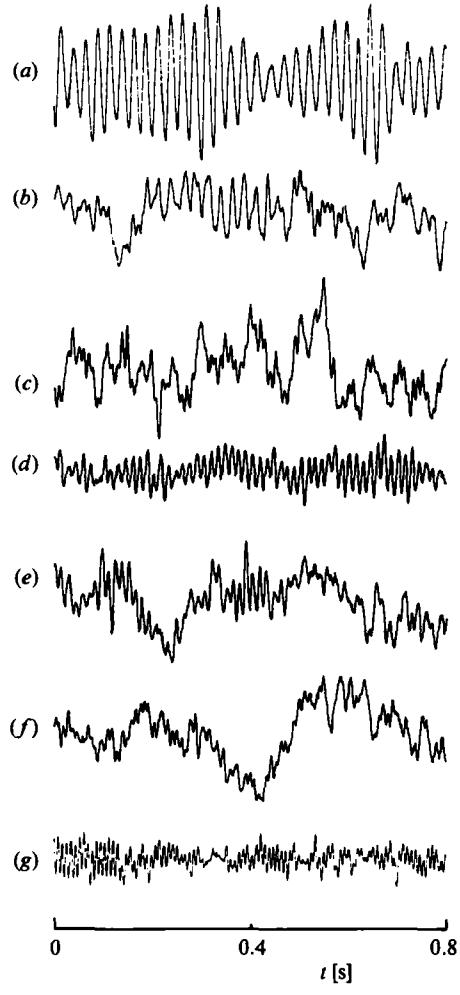

FIGURE 4. Time functions of the lift fluctuations $C_L(t)$ for Re approaching the critical values Re_{c_1} and Re_{c_2} (see also figure 3). The scale for the amplitudes is the same for all time functions (*a–g*). (*a*) Subcritical state with quasi-periodic vortex shedding, $Re/Re_{c_1} = 0.88$. (*b*) Loss of order as $Re \rightarrow Re_{c_1}$, $Re/Re_{c_1} = 0.93$; $C_L = 0$. (*c*) State immediately prior to transition *A*, $Re \approx Re_{c_1}$; $C_L = 0$. (*d*) Reordering of the flow immediately after jump *A* in the asymmetric state, $Re \approx Re_{c_1} = 0.94\, Re_{c_2}$'; $C_L = \pm 1.2$. (*e*) Loss of order again as $Re \rightarrow Re_{c_2}$, $Re = 0.99\, Re_{c_2}$. (*f*) State immediately prior to transition *B*, $Re \approx Re_{c_2}$; $C_L = \pm 0.7$. (*g*) Reordering of the flow immediately after jump *B*, the state is symmetric again. The small increase ϵ has no significant influence on the characteristics of the time function, $Re = Re_{c_2} + \epsilon$; $C_L = 0$.

regime. At critical Reynolds numbers Re_{c_1} and Re_{c_2}, transitions *A* and *B* occur if the critical values have been approached with increasing Re, which hereafter will be denoted by $Re\uparrow$. A prime on the symbol identifying the transition shall denote the phenomena occurring with decreasing Reynolds number $Re\downarrow$. Because of hysteresis effects, the corresponding transitions $A'(Re\downarrow)$ and $B'(Re\downarrow)$ occur at Re'_{c_1} and Re'_{c_2} respectively. We adjusted the flow for a critical Reynolds number by either increasing or decreasing the flow speed in very small steps. At approximately the critical value, the flow speed was held constant, and we waited a few minutes until a natural perturbation or fluctuation provoked a transition jump. This procedure

Run		1	2	3	4	5	6	7	8	9	10	11	12	13	14
sign of C_L	$Re\uparrow$	−	−	+	−	+	−	+	−	+	+	−	−	+	−
	$Re\downarrow$	+	+	+	−	−	−	+	+	+	−	+	−	+	+

TABLE 1. Distribution of the sign of the lift C_L, when the critical regime is passed 28 times

eliminated memory effects that could lead to a preference for one sign. A memory effect could involve, for example, the way in which flow speed U_∞ was accelerated to the critical Reynolds number. Under ideal conditions the transition jumps, indicated in figure 3 by arrows, would be vertical and not more or less inclined. This phenomenon can be explained by feedback effects in the closed-return wind tunnel: when the rotation speed of the fan is held constant at a critical Reynolds number, changes in the drag on the cylinder (which are coupled with a transition jump) can in turn lead to changes in the speed of the incoming flow.

The individual stages of the flow in and near the critical range may be characterized by time functions of the lift fluctuations (see figure 4). It is obvious that the flow loses stability as the Reynolds number approaches a critical value Re_{c_1} or Re_{c_2}. This tendency to lose stability can be inferred from the gradual loss of regularity in the time functions as well as from the occurrence of aperiodic low-frequency fluctuations. At Re_{c_1} and Re_{c_2}, just prior to transition, the time functions exhibit chaotic behaviour. We should note here that, in the vicinity of Re_{c_1}, the corresponding power spectra reported by Schewe (1983*a*) show two frequencies with $f_1/f_2 \approx 2.3$, which are probably incommensurate. Specifically, no period doubling has been observed. Looking at figures 3 and 4 we see that after transition A has occurred, i.e. after the time-averaged mean value $\overline{C_L(t)}$ has jumped from zero to ± 1.2, we can conclude from the reappearance of quasi-periodicity at a new vortex-shedding frequency that the flow has reordered itself. The second jump B from $C_L = \pm 0.75$ to $C_L = 0$ can be interpreted in a similar fashion. Again, the behaviour and jumps in Strouhal number are described in more detail in Schewe (1983*a*, 1985*a*).

To get an idea of the statistics of the sign of C_L, we repeated the measurements 28 times, during which the critical regime was passed 14 times for $Re\uparrow$ as well as for $Re\downarrow$ (table 1). Although the number of samples is rather small for a serious statistical study, it is still notable that the probability P for the occurrence of both signs is nearly equal, i.e. $P(+C_L) = 0.54$ and $P(-C_L) = 0.46$.

3.3. *Direct measurement of the transition jumps in the time domain*

When we consider the transition phenomena, the question arises concerning the characteristic time Δt of a transition jump and the shape of $C_L(t)$ prevailing at the instant when the jump occurs. We therefore recorded the jumps in C_L with an analyser in its transient mode. The procedure is similar to conditional sampling where the condition is provided by an internal triggering level. A trigger threshold, for example $C_L \approx 0.5$, was selected to be higher than the lift fluctuations at a critical point and lower than at the expected jump. The flow was then adjusted for a critical value Re_{c_1} or Re'_{c_2} so that a natural transition could be expected. At the instant when a transition caused the trigger level to be exceeded, the jump in $C_L(t)$ and its values immediately preceding and following transition were stored in the memory bank. Figure 5(*a*) shows a natural transition A from a symmetric subcritical state to an asymmetric state having negative sign. The measurement was taken at Re_{c_1} by

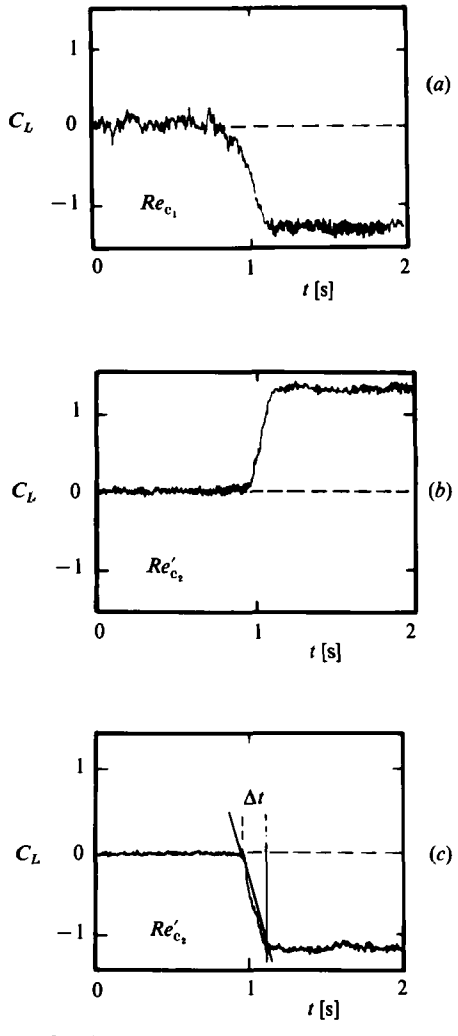

FIGURE 5. Time-dependent behaviour of the natural transition jumps $C_L(t)$ taken at fixed critical values of Re. (*a*) Jump $A\,(Re\uparrow)$ from symmetric subcritical to asymmetric state ($L/D = 10$). (*b*) Jump $B'\,(Re\downarrow)$ from symmetric supercritical to asymmetric state ($L/D = 10$). (*c*) Jump $B'\,(Re\downarrow)$ using a more slender cylinder with $L/D = 18$. A jump back to the state prior to the transition was never observed.

approaching it with increasing Reynolds number ($Re\uparrow$). Figure 5(*b*) shows a corresponding measurement taken between the supercritical and the asymmetrical state, i.e. transition $B'(Re\downarrow)$, recorded at Re'_{c_2}. After a transition had occurred in all cases the flow persisted in the new state regardless of whether the transition was from laminar to turbulent (5*a*) or from turbulent to laminar flow (5*b*). The characteristic time Δt was determined as demonstrated in figure 5(*c*), where a transition B' is shown for the more slender circular cylinder with $L/D = 18$. In figures 5(*b*, *c*), the Reynolds number and flow speed were approximately the same.

For all evaluated jumps, the characteristic time was approximately $\Delta t = 0.15$ s. This characteristic time can probably be considered to be the time required for a transition from laminar to turbulent (or from turbulent to laminar) flow to become

established along the entire cylinder. With reference to Schewe (1983*a*), it is conceivable that transition begins locally and spreads along the cylinder in a manner similar to that in a nucleation process. Therefore, making a rough approximation for the rate of spreading in the transverse direction yields $U_t = \Delta t/L \approx 4$ m/s with $U_t/U_\infty = 0.3$. This value was found in both cases, i.e. for $L/D = 10$ and 18.

Normalizing the characteristic time Δt with cylinder diameter D and flow speed U_∞ yields $\Delta t\, U_\infty/D = 34$ for $L/D = 10$ and $\Delta t\, U_\infty/D = 58$ for $L/D = 18$. These values can be compared with a typical time of the system, for example the vortex-shedding period T in the subcritical state, which is $1/Sr = TU_\infty/D \approx 5$. For the cylinder having $L/D = 10$, a typical transition thus lasts about seven shedding periods whereas, for the more slender cylinder, the number of shedding periods comparable to a transition time is about 12. Thus we can conclude that the characteristic time Δt does not scale with the vortex-shedding period T.

3.4. *Artificial tripping of transition jumps*

We were concerned in §3.3 with transition jumps where the sign of the lift force was determined by chance. In this section we shall demonstrate that it is possible to anticipate or manipulate chance by introducing a perturbation that is small compared with the dimensions of the cylinder. The perturbation used was a small movable pin of diameter $d = 0.8$ mm. This pin was installed into the surface of the circular cylinder ($D = 0.06$ m) as shown in figure 6. It was possible to extend the pin normal to the surface to various heights h by a remote-controlled stepping motor ($0 \lesssim h \lesssim 3$ mm). When in position $h = 0$, the pin is flush with a surface, i.e. there is no perturbation. The pin was positioned in the middle of the cylinder, and by turning it, the angular position ϕ of the pin can be varied. When the ratios of the characteristic sizes of the pin, the cylinder and the vortex street are considered, we see that the size of the perturbation due to the protruding pin ($h = 0.5$–1 mm) is indeed quite small ($d/D \approx 10^{-2}$ and $d/L \approx 10^{-3}$). On the other hand the size of the protruding pin and the local boundary-layer thickness are of the same order. In this context we should mention that there are at least two important lengthscales in the flow: the boundary-layer thickness on the microscopic level and the characteristic size of the evolving vortex pattern on the macroscopic level. Our artificial perturbation is small in the sense that the size of the pin is on the microscopic level while its effect will be on the macroscopic level.

The experimental procedure was as follows: as described above, the flow was adjusted to a critical value (Re_{c_1}, Re_{c_2}, Re'_{c_1} or Re'_{c_2}) so that a transition jump could be expected. Then the pin was made to protrude from the surface into the flow. In most cases, transition occurred immediately and the pin was subsequently retracted to $h = 0$. Because of hysteresis effects, the flow persisted in the new state.

We say 'in most cases', because the injection of the perturbation does not always trip the flow: in the case of transition A, it occasionally happened that transition was not established over the entire length of the cylinder. This conclusion can be drawn from the observation that, in these cases, the lift underwent a reduced jump from $C_L = 0$ to only $C_L \approx \pm 0.5$. In addition, the lift disappeared immediately as the pin was retracted. On the other hand, successive attempts to initiate transition $A'(Re\downarrow)$ and $B'(Re\downarrow)$ were nearly always successful. This point will be considered in the final discussion.

The experiments showed that, in principle, it is possible to initiate all transitions, i.e. A, A', B, B' (see figure 3), with a perturbation localized in space and time. Once a new state was established over the entire length of the cylinder, a jump back – for

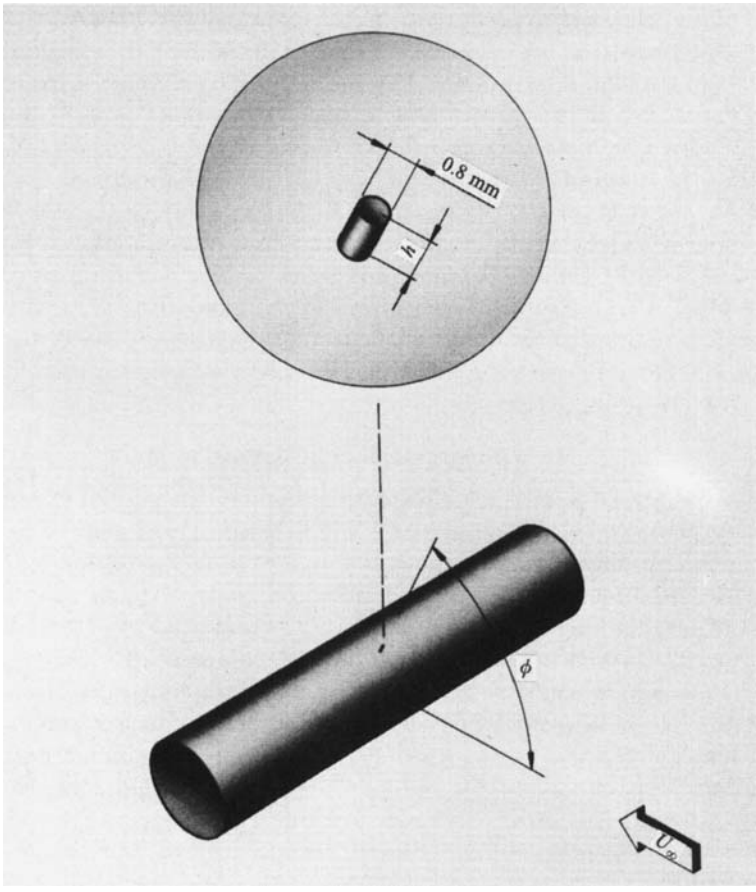

FIGURE 6. Schematic illustration of how the small perturbation works. A movable pin with diameter $d = 0.8$ mm is installed normal to the surface of the cylinder. The remote-controlled height h can be varied in the range $0 \lesssim h \lesssim 3$ mm.

example, from laminar to turbulent flow or vice versa – was never observed regardless of whether the transition was induced or natural. In all cases, the sign of the lift depended upon the angular position ϕ of the pin. Perturbing the flow on the upper side led to positive lift $(+C_L)$ if Re_{c_1} was approached with increasing Reynolds number $Re\uparrow$, and to negative lift $(-C_L)$ for Re'_{c_2} $(Re\downarrow)$. In the former case, transition A from laminar to turbulent flow in the boundary layer was initiated, while in the later case, transition B' from turbulent to laminar flow was initiated. Therefore, with the perturbation located in the same angular position ϕ, both asymmetric states can be tripped, depending on the chosen critical point as well as on how this point is approached. A perturbation on the lower side (i.e. ϕ is negative) inverts the sign.

Figures 7 (a, b) show the jumps in lift for tripped transitions $A(Re\uparrow)$ and $B'(Re\downarrow)$ recorded by using the same procedure as described for natural transitions (figures 5a, b). A direct comparison between corresponding transitions reveals that, apart from sign, there is no significant difference in the shape of the jumps regardless of whether transition is natural or induced. The minor differences found under closer examination are due to the fact that, even after the jumps had occurred, the pin was still extended during the recorded time segments shown in figure 7. Consequently, C_L is slightly reduced when compared with natural transitions. Furthermore, what

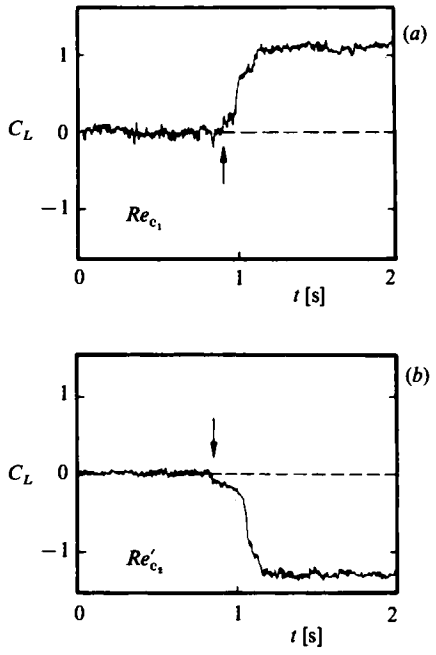

FIGURE 7. Time-dependent behaviour of transition jumps tripped by the artificial perturbation. Comparison with the corresponding jumps in figure 5 shows no significant differences. The arrows indicate the estimated start of the perturbation. After the transition jumps, the flow persisted in the new state. (*a*) Transition A ($Re\uparrow$), $h = 1$ mm, angular position of the pin $\phi = 60°$ (from Schewe 1983*b*). (*b*) Transition B' ($Re\downarrow$), $h = 0.5$ mm, $\phi = 60°$.

is the correlation in time between the protrusion of the pin and the beginning of the jump in C_L? Because of the internal triggering mode used in these experiments, this question cannot be answered exactly. We estimate that the pin was made to protrude into the flow at the instant when the short averaged lift deviated slightly from $C_L = 0$. These points in time are indicated by small arrows in figures 7 (*a*, *b*). There appears to be a time delay of about 0.1 s between the protrusion of the pin and the jump. This time delay could be interpreted as the response time needed by the system to react to the perturbation. Such a response time might be dependent upon a small deviation of the selected Reynolds number from the critical value. This interpretation should, however, be regarded as speculative since the time constant for the pin protruding from the cylinder is of the same order as the time delay. Finally, we can say that the time constant Δt of the jump itself has approximately the same value for natural transitions and for those tripped by the artificial perturbation. In addition, the height of the pin necessary for tripping the flow was $h \approx 1$ mm for transitions $A(Re\uparrow)$ and $B(Re\uparrow)$ and $h = 0.5$ mm for transitions $A'(Re\downarrow)$ and $B'(Re\downarrow)$.

In order to trip the transition, we found that the angular positions ϕ of the perturbation had to lie within the range 45–60°. What, then, is the significance of this range of angles? By using measurements of the pressure distributions $C_p(\phi)$ and wall shear stress $\tau_w(\phi)$ reported by Achenbach (1968) for Reynolds numbers near the critical value ($Re = 2.6 \times 10^5$), we find that τ_w as well as the deceleration of the fluid ($-\mathrm{d}C_p/\mathrm{d}\phi$) are high and reach their maximum in the above-mentioned range ($45° \lesssim |\phi| \lesssim 60°$). It is therefore conceivable that the efficiency of the perturbation is correlated with high values of wall shear stress and of deceleration. Also, we believe

that a perturbation introduced at $|\phi| \lesssim 45°$ will be damped by the accelerated flow in this region. For $|\phi| \gtrsim 60°$, the perturbation is perhaps ineffective because irregular fluctuations in the critical state extend down to about $|\phi| \approx 60°$.

4. Discussion of results

The transition phenomena reported in Schewe (1983*a*) can be explained as follows:

A one-sided transition from laminar to turbulent flow in the boundary layer causes the asymmetrical flow states. The process of transition from a symmetrical to an asymmetrical state (and vice versa) is coupled with the generation of circulation around the cylinder, which then causes the appearance (or disappearance) of stationary lift. Transition on one side of the cylinder probably delays transition on the other side, thus enabling the asymmetric state to stabilize itself. Only after the Reynolds number has increased noticeably does the second transition take place on the other side of the cylinder, thereby re-establishing the symmetric flow state. A more fundamental explanation of this phenomenon involves the formation of two-dimensional separation bubbles as a consequence of the transition from laminar to turbulent flow. The stationary asymmetric state is then caused by a one-sided (Bearman 1969) separation bubble, while the symmetric supercritical state is a consequence of a two-sided separation bubble. In our opinion, however, it will be sufficient to regard the transition itself as the primary cause of the phenomena described in this paper. The explanations for the phenomena will thus be simplified and also retain a more generally valid character. In addition, explanation involving two-dimensional separation bubbles can only give a rather coarse picture of reality. We have taken oil-flow photographs which show that a more or less regular three-dimensional cellular structure is formed along the cylinder. Depending upon the Reynolds number, this cellular structure is subject to drastic changes. An example of such a photograph taken by the author can be found in a paper by Dallmann (1986) who also gives an interpretation of the result.

It will be useful in the following discussion to consider the simplified schematic representation in figure 8 of the behaviour of the stationary lift-force coefficient $C_L(Re)$ in the critical range. The corresponding diagram with the measured values (figure 3) is somewhat unclear because, at each transition, feedback effects lead to a small change in Reynolds number. Figure 8 shows both hysteresis-affected transitions which (each on its own) can be interpreted as subcritical bifurcations, as were discussed and substantiated in detail by Schewe (1983*a*). The relationship between the individual states in figure 8 and the corresponding flow visualizations in figures 2(*a–e*) is indicated by symbols.

In connection with the analyses here, it is worth while to quote a description or definition of the various forms of a stability loss as formulated by Arnold (1984):

> Before the steady states loses stability the attraction domain (in phase space) becomes very small and a random perturbation can always throw the system from this domain to the other even before the attraction domain has completely disappeared. This form of loss of stability is called 'hard'. Here the system leaves its steady state with a jump to a different state of motion. This state can be another stable stationary state or a stable oscillation, or some more complex motion.

The behaviour of the flow in the critical range appears to be well described by the quotation. In the metastable range $Re'_{c_1} \lesssim Re \lesssim Re_{c_1}$ (or $Re'_{c_2} \lesssim Re \lesssim Re_{c_2}$), the attraction domain becomes steadily narrower in phase space as the Reynolds number

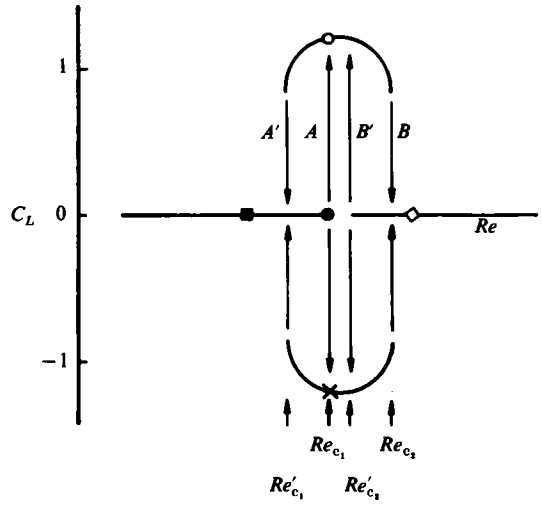

FIGURE 8. Simplified sketch of the behaviour of the steady lift coefficient C_L in the critical regime (see also figure 3). Each transition A and B can be interpreted as subcritical bifurcations. The symbols correspond to the individual states visualized in figures 2(*a–e*): ■ (*a*); ● (*b*); × (*c*); ○ (*d*); ◇ (*e*).

approaches a critical value so that a chance (or, as in our case, a premeditated) disturbance can trigger a transition. In the case of flow past a circular cylinder, there is also the fact that, at the critical points $Re_{c_1}(\uparrow)$ and $Re_{c_2}(\downarrow)$, two new stable states are available as options into which the system can jump. We can imagine that the situation in the vicinity of $Re_{c_1}(\uparrow)$ $(Re'_{c_1} \lesssim Re \lesssim Re_{c_1}, C_L = 0)$ and $Re'_{c_2}(\downarrow)$ is like a competition which becomes more feverish as the critical value (Re_{c_1} or Re'_{c_2}) is approached, and, finally, at the critical point itself, the outcome hangs in the balance. Both possibilities for the new state, characterized by the sign of C_L, have an equal chance (i.e. the same probability, see table 1) of being selected. In addition, a detailed analysis of the spectra and time functions for $Re \rightarrow Re_{c_1}$ shows that transition occurs in limited regions along the cylinder without tripping the entire system. Under these conditions, either something inherent to the system or a small external influence can deal the deciding blow and settle the outcome. In our experiment, a deciding external influence was provided by the one-sided small disturbance. After the development favouring one side has been initiated, then the process of structural changes (in our case caused by transition along the cylinder) continues because of its own internal dynamics. The disturbance can then be removed and the flow remains in the new state.

We shall close with a few comments on the statement made in §3.4 that the introduction of a local disturbance does not always initiate the transition process. We believe that, in principle, it is beyond our experimental ability to control or even recognize all contingencies that may arise in an experiment designed to study transition from laminar to turbulent vortex shedding. Although this problem is practical and not fundamental, it still has the effect of introducing a degree of uncertainty into the transition phenomena. Because of the sensitivity to small perturbations we cannot expect that such experiments as ours are reproducible in a classical sense. In the present experiment, uncertainty for example is manifested in our inability to predict the sign of the bistable state and in the arbitrarily selected time at which the artificial disturbance is introduced into the flow. At an operational

level, therefore, we can only expect to describe the artificial initiations of the transition process in terms of its probability of success.

Nevertheless the experimental results described in this paper can be summarized with the statement that in the vicinity of a critical state, a very small cause can have a very great effect.

The author drew benefit from many discussions with P. Bublitz, W. F. King, U. Dallmann and A. Lorenzen. This research was supported in part by the Deutsche Forschungsgemeinschaft (DFG).

REFERENCES

ACHENBACH, E, 1968 Distribution of local pressure and skin friction around a circular cylinder in cross flow up to $Re = 5 \times 10^6$. *J. Fluid Mech.* **34**, 625.

ARNOLD, V. I. 1984 *Catastrophe Theory*. Springer.

BEARMAN, P. W. 1969 On vortex shedding from a circular cylinder in the critical Reynolds number regime. *J. Fluid Mech.* **37**, 577.

DALLMANN, U. 1986 On the formation of three-dimensional vortex flow structures. (To be published.)

PRANDTL, L. 1914 Der Luftwiderstand von Kugeln. *Nachrichten der Gesellschaft der Wissenschaften zu Göttingen (Math.-Phys. Klasse)*, pp. 177–190.

SCHEWE, G. 1983*a* On the force fluctuations acting on a circular cylinder in crossflow from subcritical up to transcritical Reynolds number. *J. Fluid Mech.* **133**, 265–285.

SCHEWE, G. 1983*b* Über asymmetrische Strömungsablösung und deren künstliche Beeinflussung durch eine kleine Störung. In *Proc. 4.DGLR-Fachsymp. 'Strömungen mit Ablösung', Göttingen, 10–12. 10. 1983.*

SCHEWE, G. 1985*a* Experimental observation of the 'Golden Section' in flow round a circular cylinder. *Phys. Lett.* **109A**, 47.

SCHEWE, G. 1985*b* Force measurements in aerodynamics using piezo-electric multicomponent force transducers. In *Proc. 11th ICIASF '85 Record (Int. Cong. on Instrumentation in Aerospace Simulation Fac.), Stanford Univ., Aug. 26–28*, p. 263.

WIESELSBERGER, C. 1923 Versuche über den Luftwiderstand gerundeter und kantiger Körper. *Ergebnisse Aerodyn. Versuchsanstalt Göttingen* (ed. L. Prandtl), II. Lieferung, p. 23.